Catalysis Today 172 (2011) 171–176

Contents lists available at ScienceDirect

Catalysis Today

journal homepage: www.elsevier.com/locate/cattod

One-pot synthesis of olefins from aromatic ketones via tandem consecutive hydrogenation–dehydration reactions

Nicolás M. Bertero, Carlos R. Apesteguía, Alberto J. Marchi*

Catalysis Science and Engineering Research Group (GICIC), Instituto de Investigaciones en Catálisis y Petroquímica (INCAPE), FIQ-UNL, CONICET, Santiago del Estero 2654, 3000 Santa Fe, Argentina

ARTICLE INFO

Article history:
Received 24 November 2010
Received in revised form 17 April 2011
Accepted 18 April 2011
Available online 8 June 2011

Keywords:
One-pot synthesis
Tandem reactions
Hydrogenation–dehydration
Ketones
Aromatic olefins

ABSTRACT

In this work, the synthesis of aromatic olefins from the corresponding ketones via tandem consecutive hydrogenation–dehydration reactions was studied. The conversion of acetophenone (AP) to styrene (STY) was used as model reaction. Initially, the liquid-phase hydrogenation of AP to 1-phenylethanol (PHE), using cyclohexane as solvent, was investigated at 363 K and 10 bar over Ni, Co, Cu, Pd and Pt supported on SiO_2. Cu/SiO_2 was the most selective catalyst yielding 100% PHE. Then, the consecutive dehydration of PHE to STY was studied at 363 K and 2 bar over mesoporous solid acids (Al_2O_3, SiO_2–Al_2O_3, Al-MCM-41, HPA/SiO_2) and acid zeolites (HY, HBEA, HZSM-5). Zeolite HZSM-5 was the most selective catalyst, yielding 96% STY. On the basis of the former results, a mixture of Cu/SiO_2 and HZSM-5 was used to investigate the feasibility of performing the one-pot synthesis of STY from AP, by promoting tandem consecutive AP hydrogenation–PHE dehydration reactions. A maximum STY selectivity of about 72% was achieved in a two-step catalytic run: the first step was carried out at 323 K and 20 bar and the second step at 353 K and 1 bar.

1. Introduction

The synthesis of fine chemicals usually involves several consecutive-parallel reaction steps. In the case of pharmaceuticals, it is common to find synthesis processes involving between five and ten chemical reactions, whereas for agrochemicals between three and seven reactions are needed [1]. These multi-step processes often employ as many batch reactors as chemical transformations are needed in the global synthesis. This is because the successive chemical reactions are carried out separately, i.e. they are not coupled, in order to achieve the highest reaction rate and selectivity. This methodology frequently allows the successful selective synthesis of the desired product, but it involves high operative costs since every step needs to be carried out in a different reactor at specific conditions and the intermediate products have to be separated from the reaction medium after finishing each individual step. Besides, the multi-step batch processes require large volumes of solvents, salts and acid or basic liquids thereby generating a significant amount of wastes that need to be either recycled or removed [2]. Thus, it is of environmental and economic interest to develop novel integrated methodologies allowing one-pot synthesis processes via the catalytic promotion of tandem reactions. The combination of multiple reactions in single operations to increase molecular complexity enhances synthetic efficiency.

Traditionally, fine chemicals have been produced via stoichiometric processes and homogeneous catalysis, using liquid acids or bases as catalysts. In particular, the hydrogenation of aromatic ketones to alcohols and the dehydration of alcohols to olefins have been widely studied for producing fine chemicals using homogeneous catalysis. For example, the hydrogenation of aromatic ketones to alcohols has been carried out using complex metal halides such as $NaBH_4$ [3], $LiAlH_4$ [4] and KBH_4 [5] while the liquid-phase dehydration of alcohols to olefins was achieved using strong Brønsted acids such as H_2SO_4, $KHSO_4$ and p-toluenesulphonic acid [6–8]. However, all these homogeneous processes are environmentally unfriendly because of the production of a high amount of toxic, polluting and corrosive wastes.

The two-steps conversion of aromatic ketones to aromatic olefins that involves consecutive hydrogenation–dehydration reactions has also been studied for obtaining valuable products such as 2,6-dimethylnaphtalene [9,7] and indenes [5,6]. However, in these processes, the hydrogenation–dehydration sequence is carried out in two separate steps and, in some cases, using toxic and corrosive catalysts. Therefore, there is a clear need of developing one-pot processes that use efficient and eco-friendly solid catalysts for the production of fine chemicals.

Taking into account the above considerations, in this work, the use of solid catalysts for converting aromatic ketones to aromatic olefins in a one-step process via tandem

* Corresponding author. Fax: +54 342 4531068.
E-mail address: amarchi@fiq.unl.edu.ar (A.J. Marchi).

0920-5861/$ – see front matter © 2011 Elsevier B.V. All rights reserved.
doi:10.1016/j.cattod.2011.04.055

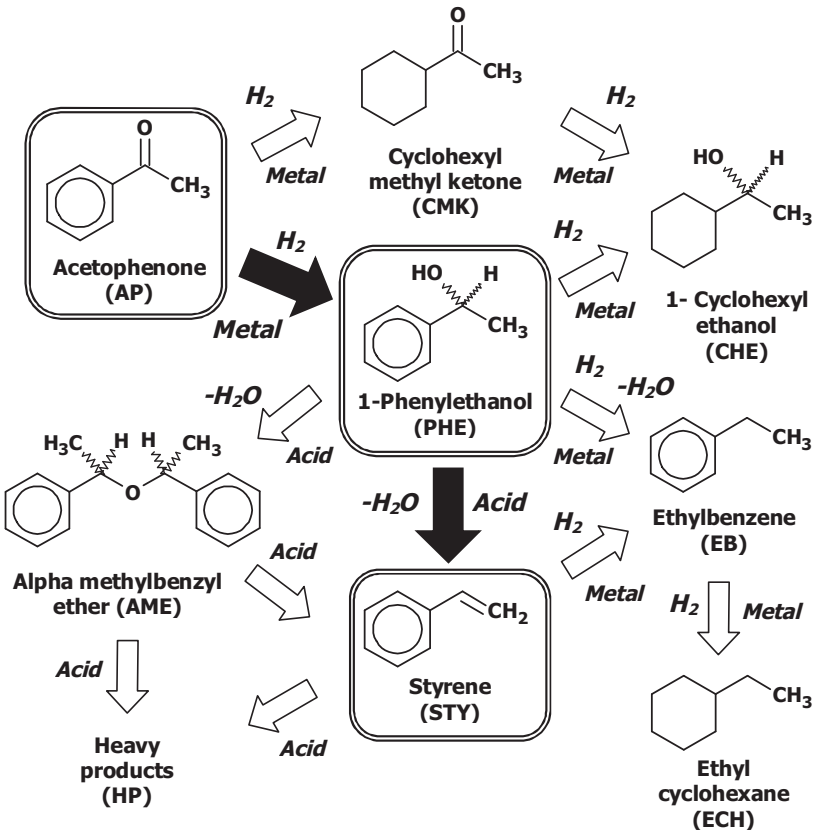

Fig. 1. Reaction network for the production of styrene from acetophenone by selective hydrogenation–dehydration sequence.

hydrogenation–dehydration reactions was investigated. Tandem reactions may be defined as a combination of two or more reactions that occur in a specific order. Three categories of tandem reactions are normally found in the literature: domino or cascade, consecutive and sequential [10]. The first class is when neither additional reagents nor changes in reaction conditions are necessary in order that all the reactions occur. If changes in either reaction conditions or addition of reagents are required to promote the tandem reactions, the terms consecutive or sequential are used, respectively [11].

In this work, the results obtained for the liquid-phase conversion of acetophenone (AP) to styrene (STY) are presented. Fig. 1 shows the reaction network for STY synthesis. The reaction pathways involved in the formation of products and byproducts over metallic and acid catalysts are shown. Selective hydrogenation of the carbonyl group of AP forms 1-phenylethanol (PHE) while reduction of the AP aromatic ring leads to cyclohexylmethylketone (CMK). Both PHE and CMK can be subsequently hydrogenated to 1-cyclohexylethanol (CHE). On the other hand, PHE can be converted to ethylbenzene (EB) by hydrogenolysis of C–OH bond. Among all these compounds, PHE is the most interesting product due to its use for the production of fragrances, flavors and pharmaceuticals [12,13]. The intramolecular PHE dehydration over acidic catalysts leads to the formation of STY. It is interesting to note that 15% of the STY worldwide production is currently obtained via PHE dehydration [14]. However, depending on the catalyst acidity and operative conditions, PHE dehydration may also produce alpha-methylbenzylether (AME). Subsequently, both STY and AME can form heavy reaction products (HP). Besides, STY in the presence of H_2 atmospheres and metal catalysts is easily hydrogenated to EB.

First, the liquid-phase AP hydrogenation and PHE dehydration reactions were studied separately in order to select the best catalysts for achieving high conversions and selectivities to PHE and STY, respectively, under mild experimental conditions. Then, the selected catalysts were used for investigating the one pot synthesis of STY from AP via tandem consecutive hydrogenation–dehydration reactions.

2. Experimental

2.1. Catalyst preparation

Ni(8%)/SiO_2, Co(8%)/SiO_2, Cu(8%)/SiO_2, Pd(0.5%)/SiO_2 and Pt(0.5%)/SiO_2 were prepared by incipient wetness impregnation adding dropwise an aqueous solution of $Ni(NO_3)_2{\cdot}6H_2O$ (Sigma–Aldrich, ≥98.5%), $Co(NO_3)_2{\cdot}6H_2O$ (Sigma–Aldrich, ≥98%), $Cu(NO_3)_2$ (Merck, 98%), $Pd(NO_3)_2$ (Merck, 99.9%) or $Pt(NH_3)_4(NO_3)_2$ (Alfa Aesar, 99.99%) over commercial silica (Grace G62, 99.7%, $S_g = 230\ m^2/g$, $V_P = 1.2\ cm^3/g$, $d_P = 20\ nm$). The impregnated samples were dried in an oven at 373 K for 12 h and then decomposed in N_2 flow at 673 K for 3 h.

HPA(28%)/SiO_2 was prepared by wet impregnation of the commercial silica (Grace G62, 99.7%) using an aqueous solution of $H_3PW_{12}O_{40}{\cdot}xH_2O$ (Merck, GR). Then, this hydrated precursor was dried in an oven at 373 K for 12 h and finally calcined in air flow at 573 K for 2 h. Commercial SiO_2–Al_2O_3 (Ketjen, LALPV, Si/Al = 11.2) and γ-Al_2O_3 (Ketjen CK-300) samples were calcined in air flow for 2 h, previous to their use in the catalytic tests, at 773 K and 573 K, respectively. Mesoporous Al-MCM-41 (Si/Al = 20) was synthesized by the sol–gel method, according to the procedure described by Edler and White [15]. After crystallization, the solid was washed with deionizated water, dried at 373 K and finally calcined at 773 K in air for 3 h.

HY zeolite was prepared by triple ion exchange of a commercial NaY zeolite (UOP-Y54, Si/Al = 2.8) using NH_4Cl (Aldrich, 99%) at

Table 1
Physicochemical properties of metal/SiO_2 catalysts.

Sample	Metal load[a] (%)	MO[b]	L_{MO}[c] (Å)	S_g[d] (m^2/g)	T_{MAX}[e] (K)	V_{H_2}[f] (l_{STP}/mol_M)	D_M (%)
Ni/SiO_2	7.6	NiO	135	245	679	0.71	6.5[g]
Co/SiO_2	7.7	Co_3O_4	131	240	578, 628	0.12	–
Cu/SiO_2	6.8	CuO	190	220	536	0.06	1.0[h]
Pt/SiO_2	0.5	–	–	243	–	2.02	16.8[g]
Pd/SiO_2	0.5	–	–	238	–	1.53	12.6[g]

[a] Determined by atomic absorption spectroscopy.
[b] Metal oxide identified by XRD.
[c] Crystallite size of metal oxide estimated applying the Debye–Scherrer equation.
[d] Specific surface area calculated using BET method.
[e] Reduction temperature at the maximum H_2 uptake in the TPR experiments.
[f] Volume of irreversibly chemisorbed hydrogen at room temperature.
[g] Estimated from irreversibly chemisorbed hydrogen assuming H/Ni = 1.
[h] Estimated by titration with N_2O at 363 K assuming $Cu/N_2O = 2$.

353 K and subsequent calcination in air at 773 K for 3 h. Commercial samples of HZSM-5 (Zeocat Pentasil PZ-2/54, Si/Al = 20) and HBEA (Zeocat PB, Si/Al = 12.5) zeolites were calcined at 773 K for 3 h in a stream of air previous to their use.

2.2. Catalyst characterization

The identification of polycrystalline species in the calcined samples was carried out by X-ray diffraction (XRD) using a Shimadzu XD-1 diffractometer and Ni-filtered Cu Kα radiation (scan speed 2°/min). Specific surface area (S_g) and mean pore diameter (d_P) were measured by N_2 physisorption at 77 K in a Quantochrome Corporation NOVA-1000 sorptometer. Elemental composition of the samples was determined by atomic absorption spectroscopy (AAS).

The reducibility of the calcined metal samples was determined by temperature-programmed reduction (TPR) using a Micromeritics AutoChem II 2920V 2.00 equipment. TPR profiles were obtained using a H_2(5%)/Ar gaseous mixture at 60 cm^3/min STP and a sample size of about 100 mg. The samples were heated from 298 to 773 K at 10 K/min. H_2 uptakes were measured using a TCD detector.

The metal dispersion of Ni/SiO_2, Pt/SiO_2 and Pd/SiO_2 catalysts was measured by hydrogen chemisorption at room temperature, whereas in the case of Cu/SiO_2 the titration with N_2O at 363 K was used [16]. Hydrogen chemisorption was measured via volumetric adsorption experiments at room temperature in a conventional vacuum apparatus using a methodology described elsewhere [17].

Acid site densities were determined by temperature-programmed desorption (TPD) of NH_3 preadsorbed at 373 K. Samples (200 mg) were treated in He (60 cm^3/min) at 773 K for 2 h and then exposed to a 1% NH_3/He stream at 373 K. Weakly adsorbed NH_3 was removed by flowing He at 373 K during 2 h. Temperature was then increased at 10 K/min and the NH_3 concentration in the effluent was measured by mass spectrometry (MS) using a Baltzers Omnistar unit. The position of the desorption bands (maximum temperature) was associated with the acid strength whereas the intensity of the bands (area of the peak) was used to estimate the surface acid site density.

The nature of surface acid sites was determined by Fourier transform infrared spectroscopy (FTIR) with a Shimadzu FTIR-8101M spectrophotometer, by using pyridine as probe molecule and in the range 1400–1700 cm^{-1}. Sample wafers were formed by pressing 20–40 mg of the catalyst at 5 tons/cm^2 and transferred to a sample holder made of quartz. An inverted T-shaped Pyrex cell containing the sample pellet was used. All the samples were initially outgassed at 723 K for 4 h and then a background spectrum was recorded after cooling the sample at room temperature. Data were obtained after admission of pyridine, adsorption at room temperature and evacuation at 423 K for 30 min. Spectra were always recorded at room temperature. The pyridine adsorption bands at around 1540 cm^{-1} and between 1440 and 1460 cm^{-1} were considered to account for pyridine adsorbed on Brønsted (B) and Lewis (L) sites, respectively [18]. The relative contributions of L and B acid sites were obtained by deconvolution and integration of these pyridine absorption bands.

2.3. Catalytic tests

The liquid-phase hydrogenation of AP (Aldrich, 99%) and the dehydration of PHE (Aldrich, 99%) were carried out in a 600 ml autoclave (Parr 4843), equipped with mechanical stirrer, in the range of 353–373 K and using cyclohexane (Merck, 99%) as solvent. The autoclave was loaded with 150 ml of solvent and 0.5–1 g of catalyst. The catalytic samples were either calcined or activated ex situ and transferred into the reactor under inert atmosphere (N_2). The reaction system was stirred and heated up to reaction temperature at 2 K/min. Then, 1.5–4.5 ml of AP or PHE, depending on the experiment, were injected to the reactor and the pressure was rapidly increased up to either 10 bar with H_2, for hydrogenation or one-pot experiments, or 2 bar with N_2, for dehydration experiments. The batch reactor was assumed to be perfectly mixed. A stirring speed of 600 rpm and catalyst particles less than 100 μm in size were used to insure the kinetic control of the reaction; i.e. diffusional limitations were negligible [19,20]. Concentrations of reactants and products were followed during the reaction by ex situ gas chromatography using an Agilent 6850 chromatograph equipped with flame ionization detector heated at 523 K, temperature programmer and a 30 m Innowax capillary column with a 0.25 mm coating. Liquid samples were withdrawn from the reactor by using a loop under pressure in order to avoid flushing. Reactant conversion (X_j, j = AP, PHE, mol of j reacted/mol of j fed) was calculated as $X_j = (C_j^0 - C_j)/C_j^0$; where C_j^0 is the initial concentration of reactant and C_j is the reactant concentration at reaction time t. Selectivities towards product i (S_i, mol of product i/mol of converted reactant) were calculated as $S_i = C_i/\sum C_i$, where $\sum C_i$ is the product total concentration. The C_i values were calculated using n-dodecane (Sigma–Aldrich, >99%) as internal standard. Yields (Y_i, mol of product i/mol of reactant fed) were calculated as $Y_i = S_i X_j$.

3. Results and discussion

3.1. AP hydrogenation

Table 1 presents the characterization results obtained for supported metal catalysts. After the activation process, all the catalysts were of the kind M^0/SiO_2 (M = Ni, Co, Cu, Pt, Pd). The specific surface area (S_g) of the catalysts did not differ greatly from that of SiO_2 support (230 m^2/g). Metal dispersion, determined by H_2 chemisorption, was within 2 and 17% for all the samples. The capac-

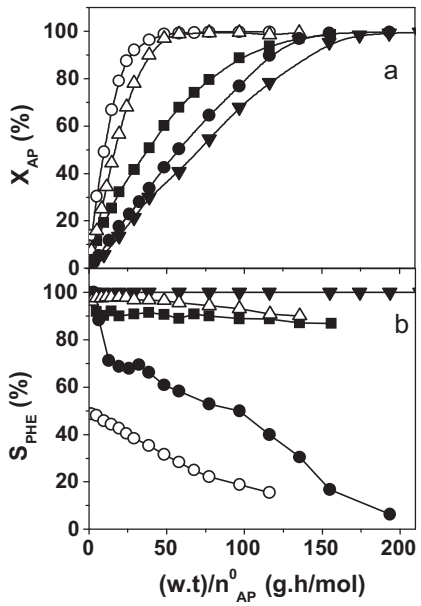

Fig. 2. Acetophenone hydrogenation over metal/SiO_2 catalysts: (○) Pt/SiO_2; (△) Pd/SiO_2; (■) Ni/SiO_2; (●) Co/SiO_2 and (▼) Cu/SiO_2. (a) Acetophenone conversion (X_{AP}); (b) selectivity to 1-phenylethanol (S_{PHE}) [363 K, 10 bar (H_2), 0.5–1 g catalyst, AP/solvent = 1/50 vol., solvent: cyclohexane].

ity for irreversible H_2 chemisorption (Table 1) followed the pattern: Pt > Pd > Ni ≫ Co > Cu, showing a large difference between noble metal and non-noble metal based catalysts.

Cyclohexane was chosen as the reaction solvent due to its weak interaction with the reactants and also because of its almost negligible adsorption on metals [19] and weak adsorption over solid acids [21]. Results on catalyst activity and selectivity for AP hydrogenation on metal/SiO_2 samples are shown in Fig. 2. These results are given as a function of $w.t/n^0_{AP}$, where w is the catalyst weight, t the reaction time and n^0_{AP} the initial moles of the reactant. The AP conversion rate clearly followed the pattern: Pt/SiO_2 > Pd/SiO_2 > Ni/SiO_2 > Co/SiO_2 > Cu/SiO_2 (Fig. 2a), in agreement with the pattern obtained for the H_2 chemisorption capacity on these samples (Table 1). On the other hand, the selectivity pattern towards PHE was: Cu/SiO_2 > Pd/SiO_2 > Ni/SiO_2 > Co/SiO_2 > Pt/SiO_2 (Fig. 2b). Initially, Pt/SiO_2 produced similar amounts of PHE and CMK so that the initial selectivity to PHE was 50%. Then, PHE was converted into CHE by hydrogenation of the aromatic ring and thus selectivity to PHE diminished with the progress of the reaction. In contrast, Pd/SiO_2 showed a high initial selectivity to PHE that decreased later by the hydrogenolysis of PHE to EB. On non-noble metal catalysts, the initial selectivity to PHE was near to 100% in all the cases. Ni/SiO_2 hydrogenated AP mainly to PHE but also formed CMK. Both primary products were then consecutively hydrogenated to CHE. In contrast, Co/SiO_2 did not hydrogenate the aromatic ring of AP and produced initially only PHE. However, PHE was rapidly converted by hydrogenolysis to EB. Finally, Cu/SiO_2 was the most selective catalyst towards PHE. Neither hydrogenation of the aromatic ring in AP nor hydrogenolysis/hydrogenation of PHE was observed, in agreement with previous results [19]. The PHE selectivity on Cu/SiO_2 was 100% during the complete catalytic run (Fig. 2b).

In summary, Cu/SiO_2, having the lowest capacity for irreversible H_2 chemisorption, was the less active but the most selective catalyst to obtain PHE from AP.

3.2. PHE dehydration

The characterization results for the acidic catalysts are presented in Table 2. The pore volume diminution observed after impregnation of SiO_2 with HPA suggested the partial blocking of SiO_2 pores. The XRD pattern of Al-MCM-41 sample showed a strong diffraction peak at 2.2°, corresponding to (1 0 0) reflection, and two weaker peaks at 3.7° and 4.3°, corresponding to (1 1 0) and (2 0 0) reflections. This confirmed the hexagonal structure of mesoporous Al-MCM-41 [15]. Regarding the zeolite characterization, it was verified by N_2 physisorption at 77 K and XRD that the crystalline structure and specific surface area of all of the zeolites used in this work were preserved after the calcination process. Furthermore, the crystallinity degree was higher than 85% in all the cases.

The acid properties of the samples were probed by TPD of NH_3 preadsorbed at 373 K and FTIR spectroscopy of adsorbed pyridine (Table 2). The density and strength of surface acid sites of these samples were markedly different and, as a consequence, presented different activity for PHE dehydration as it can be observed in Fig. 3. The initial PHE conversion rates (r^0_{PHE} mol/g min) were calculated by polynomial differentiation at time zero of X_{PHE} vs time curves (Fig. 3); the obtained r^0_{PHE} values for the most active samples are shown in Table 3. Similarly, the initial formation rates for STY and AME were calculated by polynomial differentiation of the Y_i vs time curves (not shown here) at time zero to determine the initial selectivities that are given in Table 3.

γ-Al_2O_3 contained only weak Lewis acid sites (Table 2) and was practically inactive for PHE dehydration (Fig. 3a). Al-MCM-41, with a high proportion of Brønsted acid sites of medium strength (Table 2), was active and initially selective to AME. Then, STY was formed as secondary reaction product from AME but the maximum STY yield was only about 20% (Table 3). Over SiO_2–Al_2O_3, with a similar proportion of Brønsted to Lewis acid sites than Al-MCM-41

Table 2
Characterization of solid acid catalysts.

Sample	Si/Al[a]	S_g[b] (m^2/g)	V_P (cm^3/g)	D_P[c] (Å)	NH_3 TPD		L/(L+B)[f]
					T[d] (K)	δ[e] (μmol/m^2)	
HPA/SiO_2	–	205	0.61	220[c]	423–1173	0.80	0.20
SiO_2–Al_2O_3	11.2	536	0.74	50[c]	433–773	0.60	0.75
Al-MCM-41	20	925	0.68	30[c]	463–723	0.40	0.81
Al_2O_3	0	160	0.25	41[c]	421–610	0.11	1.00
HBEA	12.5	560	0.17	6.6 × 6.7; 5.6 × 5.6	463–763	0.89	0.55
HZSM-5	20.0	350	0.16	5.1 × 5.5; 5.3 × 5.6	483–493; 573–773	2.20	0.50
HY	2.4	660	0.26	7.4	483–493; 573–773	2.09	0.60

[a] Determined by atomic absorption spectroscopy.
[b] Specific surface area calculated using BET method.
[c] Pore diameter estimated by BJH method.
[d] Ammonia desorption temperature range determined by NH_3 TPD.
[e] Acid site density determined by NH_3 TPD.
[f] Ratio of Lewis to Brønsted sites determined by FTIR of adsorbed pyridine.

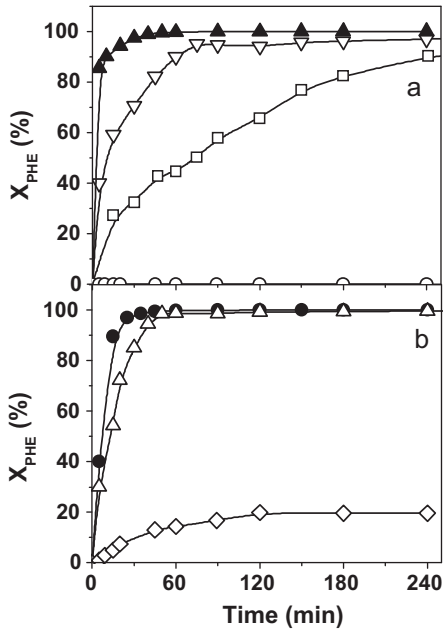

Fig. 3. Dehydration of 1-phenylethanol over acid catalysts. 1-phenylethanol conversion (X_{PHE}) over (a) mesoporous oxides: (▲) HPA/SiO_2; (▽) SiO_2–Al_2O_3; (□) Al-MCM-41 and (○) Al_2O_3 and (b) zeolites: (●) HBEA; (Δ) HZSM-5 and (◊) HY [363 K, 2 bar (N_2), 0.5 g catalyst, PHE/solvent = 1/50 vol., solvent: cyclohexane].

(Table 2), only AME was formed as primary product as well. Then, STY and small amounts of HP were produced from AME with the progress of the reaction; the maximum Y_{STY} on SiO_2–Al_2O_3 was 38% (Table 3). HPA/SiO_2 contained essentially strong Brønsted acid sites (Table 2) and was the most active catalyst, producing initially mainly AME from PHE. However, after 4 h, the final reaction products were mainly HP formed from STY and AME (Table 3). This result showed that the formation of HP is promoted by the presence of strong Brønsted acid sites.

Zeolites HY, HBEA and HZSM-5 contained a similar L/(L + B) acid sites ratio (between 0.5 and 0.6) and showed the highest initial selectivities to STY (Table 3). However, zeolite HY was rapidly deactivated reaching only 20% of PHE conversion (Fig. 3b); probably HP formation inside the cages blocks the microporous structure of zeolite HY causing the rapid catalyst deactivation [22]. The initial STY selectivity on zeolite HBEA was 96%, but increasing amounts of HP were formed as the reaction proceeded and the STY selectivity decreased to 73% at the end of the run (Table 3). In contrast, zeolite HZSM-5 was very stable and selective, yielding 96% of STY (Table 3). The superior selectivity and stability observed on zeolite HZSM-5 for PHE dehydration may be explained by considering that the narrow channels of this zeolite avoid the formation of AME and other heavier products [20].

In summary, results presented in Fig. 3 and Table 3 show that zeolite HZSM-5 has the appropriate textural and acid properties to convert selectively PHE to STY under mild operative conditions.

Table 3
Catalytic performance for PHE dehydration on the most active acid samples.

Sample	r^0_{PHE} [a] (mol/g min)	S^0_{STY} [b]	Y_{STY} [c]
HPA/SiO_2	6.56×10^{-3}	0.10	0.21
SiO_2–Al_2O_3	2.47×10^{-3}	0.02	0.38
Al-MCM-41	6.66×10^{-4}	0.02	0.21
HBEA	3.04×10^{-3}	0.96	0.73
HZSM-5	1.89×10^{-3}	0.94	0.95

[a] Initial conversion rate of 1-phenylethanol.
[b] Initial selectivity to styrene calculated as r^0_{STY}/r^0_{PHE}.
[c] Styrene yield at the end of catalytic runs.

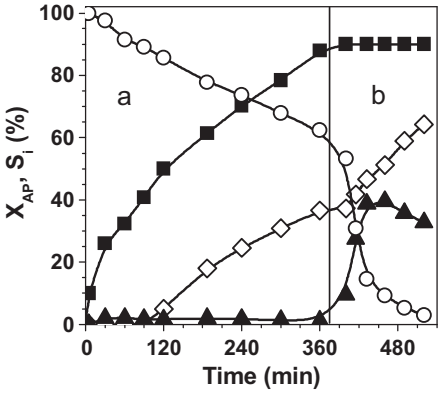

Fig. 4. Tandem hydrogenation–dehydration reactions: (■) acetophenone conversion (X_{AP}) and selectivities (S_i) to (○) PHE, (▲) STY and (◊) EB. Reactor loaded with AP/cyclohexane = 1/50 vol. and a mechanical mixture of Cu/SiO_2 (1 g) and HZSM-5 (0.5 g). (a) First step [333 K, 10 bar (H_2)]; (b) second step [353 K, 1 bar (H_2)].

3.3. One-pot styrene synthesis from acetophenone

Previously to the tandem reactions, it was verified that some possible undesirable reactions, as for example aldol condensation of AP and STY oligomerization, do not take place over HZSM-5 in the conditions used in this work.

The one-pot synthesis of STY from AP via the tandem consecutive hydrogenation–dehydration reactions depicted in Fig. 1 was studied using a mechanical mixture of Cu/SiO_2 and HZSM-5. These two catalysts were selected following the catalytic tests performed for individual hydrogenation and dehydration reactions, as detailed above. Initially, an exploratory catalytic run was performed at 363 K and 10 bar of H_2, loading the reactor with AP and the catalyst mechanical mixture. The only reaction product detected from the very beginning was EB. This is indicating that PHE, produced by AP hydrogenation over Cu/SiO_2, was rapidly dehydrated on HZSM-5 to STY which was in turn hydrogenated faster to EB over Cu/SiO_2. Similar selective EB formation was observed using a bifunctional Cu/HZSM-5 catalyst, prepared by incipient wetness impregnation.

In order to promote the preferential formation of STY, the reaction conditions were changed by taking into account previous information on the kinetics of AP hydrogenation over Cu/SiO_2 and PHE dehydration over HZSM-5. In fact, the apparent activation energies for AP hydrogenation to PHE over Cu/SiO_2 and PHE dehydration to STY over HZSM-5 are approximately 54.9 kJ/mol and 95.2 kJ/mol, respectively [19,20]. Thus, the PHE dehydration rate will decrease more than the AP hydrogenation rate with the diminution of reaction temperature. On the other hand, it has to keep in mind that the undesirable hydrogenation of STY to EB may be controlled by drastically diminishing the reactor H_2 pressure. Taken into account all these considerations, we performed a second catalytic run in two steps. The first step was carried out at 333 K and 10 bar of H_2 (Fig. 4a). When the AP conversion reached about 90%, the H_2 pressure was suddenly diminished to 1 bar and the temperature increased to 353 K (Fig. 4b). The formation of STY rapidly increased reaching about 40% selectivity when PHE was totally consumed. This result revealed that decreasing the H_2 pressure and raising the temperature in a second step, seems to be a good procedure to increase the STY selectivity. However, Fig. 4a shows that formation of EB was significant in the first step performed at 333 K and 10 bar. In fact, at the end of the first step the selectivity to EB was approximately 35%, which is detrimental for enhancing STY yield.

Based on the results of Fig. 4 and by considering that the AP hydrogenation over Cu/SiO_2 is order one with respect to H_2 [19], a third catalytic run was carried out by changing the reaction con-

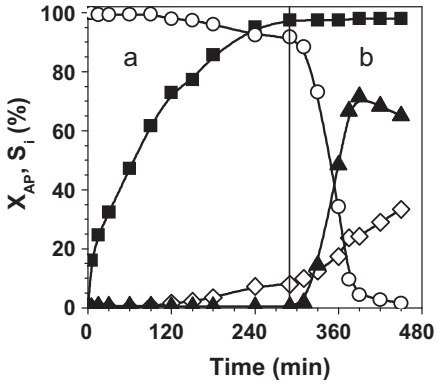

Fig. 5. Tandem hydrogenation–dehydration reactions: (■) acetophenone conversion (X_{AP}) and selectivities (S_i) to (○) PHE, (▲) STY and (◊) EB. Reactor loaded with AP/cyclohexane = 1/50 vol. and a mechanical mixture of Cu/SiO_2 (1 g) and HZSM-5 (0.5 g). (a) First step [323 K, 20 bar (H_2)]; (b) Second step [353 K, 1 bar (H_2)].

ditions of step 1 to $T = 323$ K and $P_{H_2} = 20$ bar with the aim of diminishing the EB formation rate. Results are given in Fig. 5. The selectivity to EB was lower than 10% at the end of the first step, when AP conversion reached 95% (Fig. 5a). Then, the second step was performed at the same operative conditions than in Fig. 4b, i.e. $T = 353$ K, $P_{H_2} = 1$ bar, in order to favor PHE dehydration on HZSM-5 against STY hydrogenation on Cu/SiO_2 (Fig. 5b). It was observed that the formation of STY rapidly increased in this second step; the S_{STY} value attained 72% when PHE was completely consumed. This result shows that the one-pot synthesis of styrene from acetophenone may be efficiently achieved via tandem consecutive hydrogenation–dehydration reactions by changing operative conditions to assure the correct propagation of the reaction sequence. It deserves to be noticed that even when acetophenone was chosen as a probe molecule in this work, it is expected that the catalysts and the reaction conditions employed here may be successfully extrapolated to promote the synthesis of olefins from aromatic ketones of similar structure than acetophenone.

4. Conclusions

The one-pot synthesis of styrene from acetophenone in liquid-phase may be efficiently promoted via tandem consecutive hydrogenation–dehydration reactions using a mechanical mixture of Cu/SiO_2 and zeolite HZSM-5. To obtain high styrene yields, it is required to change the operative conditions in a two-step catalytic run for assuring the correct propagation of the reaction sequence. In the first step, high H_2 pressure and low reaction temperature favor the selective ketone hydrogenation to the corresponding aromatic alcohol over Cu/SiO_2 and diminish the subsequent alcohol dehydration over the acid catalyst. In the second step, the H_2 pressure must be reduced and the temperature increased in order to promote the alcohol dehydration over HZSM-5 and to diminish the olefin hydrogenation over Cu/SiO_2 catalyst. This methodology would allow the synthesis of aromatic olefins used in Fine Chemistry employing an eco-friendly catalytic process under mild conditions.

Acknowledgements

We thank the Universidad Nacional del Litoral (UNL), Consejo Nacional de Investigaciones Científicas y Técnicas (CONICET) and Agencia Nacional de Promoción Científica y Tecnológica (ANPCyT), Argentina, for the financial support to this work.

References

[1] H.U. Blaser, Catal. Today 60 (2000) 161–165.
[2] R.A. Sheldon, Chem. Ind. (1992) 903–906.
[3] J.D. Prugh, A.W. Alberts, A.A. Deanna, J.L. Gilfillian, J.W. Huff, R.L. Smith, J.M. Wiggins, J. Med. Chem. 33 (1990) 758–765.
[4] M. Olivier, E. Maréchal, Bull. Soc. Chim. Fr. (1973) 3092–3096.
[5] D.R. Buckle, J.R.S. Arch, C. Edge, K.A. Foster, C.S.V. Houge-Frydrych, I.L. Pinto, D.G. Smith, J.F. Taylor, S.G. Taylor, J.M. Tedder, R.A.B. Webster, J. Med. Chem. 34 (1991) 919–926.
[6] C.L. Becker, M.L. McLaughlin, Synlett (1991) 642–1642.
[7] T. Abe, S. Ebata, H. Machida, K. Kida, US Patent 5,023,390, Mitsubishi Gas Chemical Company Inc. (1991).
[8] N. Piccolrovazzi, P. Pino, G. Consiglio, A. Sironi, M. Moret, Organometallics 9 (1990) 3098–3105.
[9] T. Abe, S. Uchiyama, T. Ojima, K. Kida, US Patent 5,008,479, Mitsubishi Gas Chemical Company Inc. (1991).
[10] S.E. Denmark, A. Thorarensen, Chem. Rev. 96 (1996) 137–165.
[11] T. Ho, Tandem Organic Reactions, Wiley-Interscience, New York, 1992.
[12] M.V. Rajashekharam, I. Bergault, P. Fouilloux, D. Schweich, H. Delmas, R.V. Chaudhari, Catal. Today 48 (1999) 83–92.
[13] A. Drelinkiewicza, A. Waksmundzka, W. Makowski, J.W. Sobczak, A. Król, A. Zieba, Catal. Lett. 94 (2004) 143–156.
[14] K. Weissermel, H.J. Arpe, Industrial Organic Chemistry, 4 ed., Wiley-VCH, 2003.
[15] K.J. Edler, J.W. White, Chem. Mater. 9 (1997) 1226–1233.
[16] A. Dandekar, M.A. Vannice, J. Catal. 178 (1998) 621–639.
[17] A.J. Marchi, J.F. Paris, N.M. Bertero, C.R. Apesteguía, Ind. Eng. Chem. Res. 46 (2007) 7657–7666.
[18] A. Corma, C. Corell, V. Fornés, W. Kolodziejski, J. Pérez-Pariente, Zeolites 15 (1995) 576–582.
[19] N.M. Bertero, C.R. Apesteguía, A.J. Marchi, Appl. Catal. A: Gen. 349 (2008) 100–109.
[20] N.M. Bertero, C.R. Apesteguía, A.J. Marchi, Catal. Commun. 10 (2009) 1339–1344.
[21] J.A. Miller, W.C. Comer, J. Phys. Chem. 97 (1993) 1451–1454.
[22] N. Lavaud, P. Magnoux, F. Alvarez, L. Melo, G. Giannetto, M. Guisnet, J. Mol. Catal. A: Chem. 142 (1999) 223–236.